TISSUE ENGINEERING: Part A
Volume 15, Number 12, 2009

DOI: 10.1089/ten.tea.2008.0594

The Potential of Nanoporous Anodic Aluminium Oxide Membranes to Influence Skin Wound Repair

Leigh G. Parkinson, B.Sc.(Hons),[1,2] Natalie L. Giles, Ph.D.,[2] Katharine F. Adcroft, B.Sc.(Hons),[2] Mark W. Fear, Ph.D.,[2] Fiona M. Wood, M.B.,[2–4] and Gerard E. Poinern, Ph.D.[1]

Cells respond to changes in the environment by altering their phenotype. The ability to influence cell behavior by modifying their environment provides an opportunity for therapeutic application, for example, to promote faster wound healing in response to skin injury. Here, we have modified the preparation of an aluminium oxide template to generate large uniform membranes with differing nano-pore sizes. Epidermal cells (keratinocytes) and dermal cells (fibroblasts) readily adhere to these nanoporous membranes. The pore size appears to influence the rate of cell proliferation and migration, important aspects of cell behavior during wound healing. The suitability of the membrane to act as a dressing after a burn injury was assessed *in vivo*; application of the membrane demonstrated adherence and conformability to the skin surface of a pig, with no observed degradation or detrimental effect on the repair. Our results suggest that keratinocytes are sensitive to changes in topography at the nanoscale level and that this property may be exploited to improve wound repair after tissue injury.

Introduction

The skin is the largest organ of the human body, providing a protective barrier against the environment and serving several homeostatic and sensory functions vital to an individual's well-being. When areas of skin are lost through trauma, disease, or surgery, the increase in susceptibility to infection, together with the loss of blood, fluid, and essential salts, creates a need for rapid repair. Although modern medicine has drastically reduced mortality associated with significant skin injury, the scars resulting from the repair process continue to significantly affect the quality of life of patients after recovery.

Tissue regeneration, rather than enhanced repair, remains the ultimate goal of wound healing research. However, the degree of scarring and the quality of the repair depend on the time taken to heal, with faster healing correlating to improved outcome.[1] This has led to the development of and increased interest in tissue engineering technologies that may provide wound cover in shorter time frames.

Cells respond to changes in their environment by altering their phenotype.[2–4] Therefore, technologies that enhance the environment for wound healing are critical to reducing scar formation and improving outcome. Several approaches to wound environment optimization have already been used in the wound healing field.[5] For example, dermal scaffolds such as Integra (Integra Life Sciences, Plainsboro, NJ) and Apligraf (Organogenesis, Canton, MA) are thought to provide appropriate topography and matrix properties to promote cell migration into the wound, improve healing, and reduce scarring.[6–8]

The development of improved scaffolds or templates to enhance repair has been the main focus of the tissue engineering field. One area of investigation has concentrated on the effect of topography on cell response and the ability to elicit control over cells using surface detail. There is extensive evidence of the importance of micro-meter-sized features in modulating cell behavior, with cells responding to physical cues through a phenomenon known as "contact guidance."[9–12] With the evolution of nanotechnology, areas of cell research have shifted to explore the role of nanoscale detail on cell function. The existence of many nanoscale structures on cell surfaces with roles in attachment and migration and important nano-architectural frameworks *in vivo* has led to greater interest in nanostructured surfaces and their potential use in tissue engineering.[11–19]

The types of nanotopographical features that can be fabricated have been divided into two main categories—unordered and ordered topographies.[19] Many of the current scaffolds or templates are unordered topographies and are generally matrices of synthetic and natural polymers, fabricated using various techniques, including solvent-casting,

[1]Department of Physics and Nanoscience, School of Engineering and Energy, Murdoch University, Perth, Australia.
[2]McComb Research Foundation, Perth, Australia.
[3]School of Surgery, University of Western Australia, Perth, Australia.
[4]Burns Service WA, Royal Perth Hospital and Princess Margaret Hospital, Perth, Australia.

gas foaming, phase separation or polymer demixing, freeze drying, melt molding, and solid free-form fabrication.[16–24] However, these biopolymer scaffolds tend to encounter problems such as poor reproducibility because of the lack of control over pore size and feature geometry, residual toxic organic solvents, and the potential to elicit inflammatory and immune responses due to polymer degradation and the associated by-products.[20,21] Techniques such as electron beam lithography have been used to fabricate highly ordered nanostructured surfaces, but the production of large and reproducible areas is costly and time consuming and requires a high level of expertise. A low-cost, reproducible model substrate with large areas of controlled nanotopography is necessary to allow for a systematic study of cell response and application in tissue engineering.

Anodic aluminium oxide (AAO) has potential to act as a scaffold or template in tissue engineering.[25–30] It possesses a highly regular, porous structure produced from the anodic oxidation of aluminium in acidic electrolytes. Under controlled conditions, the self-organized oxide growth generates a densely packed hexagonal array of uniform-sized nanopores that are almost perfectly aligned perpendicular to the surface of the AAO film.[31,32] Nanoengineering of the pore geometry can be achieved simply by changing macroscopic parameters, such as the anodization time and voltage, the anodizing electrolyte, and the time of postchemical etching.[33–35] Essentially, the system provides the ability to manufacture specific nanotopographies for specific applications. Aluminium oxide is also well known for its biocompatibility in the human body,[36,37] and its inert, stable, nonreactive nature overcomes some of the common problems associated with polymer scaffolds. The cost of producing AAO membranes remains low, and the ease and reproducibility of the membrane production by controlling macroscopic parameters means that AAO membranes have the potential to provide a cheap and consistent nanostructured substrate for large-scale tissue engineering and studies of cell response.

We developed highly regular nanoporous AAO films with high consistency, reproducibility, and quality and of sizes up to 56 cm^2, with a range of pore sizes between 40 and 500 nm. We then studied the effects of pore size on the attachment, growth, and migration of immortalized human skin cell lines—keratinocyte (HaCaT cell line) epidermal cells and the fibroblast (NIH-3T3) dermal cell lines—using standard tissue culture conditions. The cells readily attach to nanoporous AAO membranes, and the rate of proliferation changes in response to alteration in the pore size. Keratinocyte migration across the nanostructured surfaces was also different depending on the pore size. In summary, skin cells appear to be sensitive to nanoscale changes in topography, and manipulation of the nanotopography of these surfaces may provide an improved template for promoting rapid wound repair after cutaneous injury. The membrane could potentially be used as a dressing to promote epithelial cover or as a delivery vehicle template for an "upside-down transplantation" of cells with enhanced function.

Materials and Methods

Nanoporous alumina fabrication

The process of fabricating regular nanoporous AAO is schematically summarized in Figure 1. A custom-made apparatus allowed the fabrication of superior large-scale membranes of 56 cm^2 from the anodization of a single side of high-purity aluminium. First, aluminium foil discs were annealed under argon at 500°C for 5 h to recrystallize and release mechanical stresses from the samples. The substrates were degreased in acetone and etched in sodium hydroxide (3M) for 5 min before thorough washing with milli-Q water. AAO membranes were fabricated using an advanced two-step anodization process.[32] A first anodization step was performed in an oxalic acid electrolyte (0.3 M, 5°C, mechanically stirred) at a constant direct current voltage of 30 V for 7 h (Fig. 1a). The sample was then exposed to a mixture of phosphoric and chromic acid (70 mL/L and 20 g/L, respectively) at 60°C for 1 h to selectively remove the alumina layer formed on the unprotected side of the sheet and expose the textured substrate for the second anodization step (Fig. 1b). A second anodization was performed for 14 h under the same conditions as the first (oxalic acid, 0.3 M, 5°C, 30 V), resulting in a regular, honeycomb arrangement of nanopores, extending parallel throughout the layer (Fig. 1c). The nanopores were then widened using chemical etching in phosphoric acid (5%) at 35°C for 7 min (Fig. 1d). A thin and even coat of Acrifix 192 (Röhm GmbH & Co. KG. Darmstadt, Germany), a liquid acrylic product, was applied to the anodized side of the strip (Fig. 1e). The acrylic film serves to support the AAO membrane during removal of the aluminium substrate using a copper chloride ($CuCl_2$)-based solution (0.1M $CuCl_2$ in 7% hydrochloric acid) (Fig. 1f). Etching of the barrier layer oxide in phosphoric acid (Fig. 1g) and complete dissolution of the acrylic support in acetone resulted in the AAO membrane as a clear thin film (Fig. 1h). Sets of different anodization conditions were employed to fabricate AAO membranes with differing pore sizes. These are described in Table 1.

Before use in cell experiments, the alumina membranes were cleaned in hot hydrogen peroxide (30%) for 15 min and then thoroughly washed in sterile milli-Q water.

Surface characterization

A Philips XL30 scanning electron microscope (SEM, FEI Company, Hillsboro, OR) was used to quantitatively study AAO surface topography and pore geometry. Samples were sputter-coated with gold at room temperature and visualized at various magnifications at 10 to 15 kV.

AAO topography was also characterized using atomic force microscopy (AFM), using a Digital Nanoscope E instrument (Digital Instruments/Veeco, Plainview, NY). AFM scans were collected with microfabricated silicon cantilevers with silicon nitride–sharpened tips operated in contact mode. Images were recorded and 'flattened' to correct for the inherent curvature of the AFM scanner using Nanoscope III Digital Instruments Software version 5.12r^3 (Veeco, Plainview, NY).

Cell culture

The immortalized HaCaT cell line was used for epidermal cell experiments, and the NIH-3T3 fibroblast cell line was used for dermal cell experiments. The HaCaT cell line is a spontaneously immortalized keratinocyte cell line that retains the characteristics of primary human keratinocytes.[38] Cells were cultured in Dulbecco's modified Eagle medium

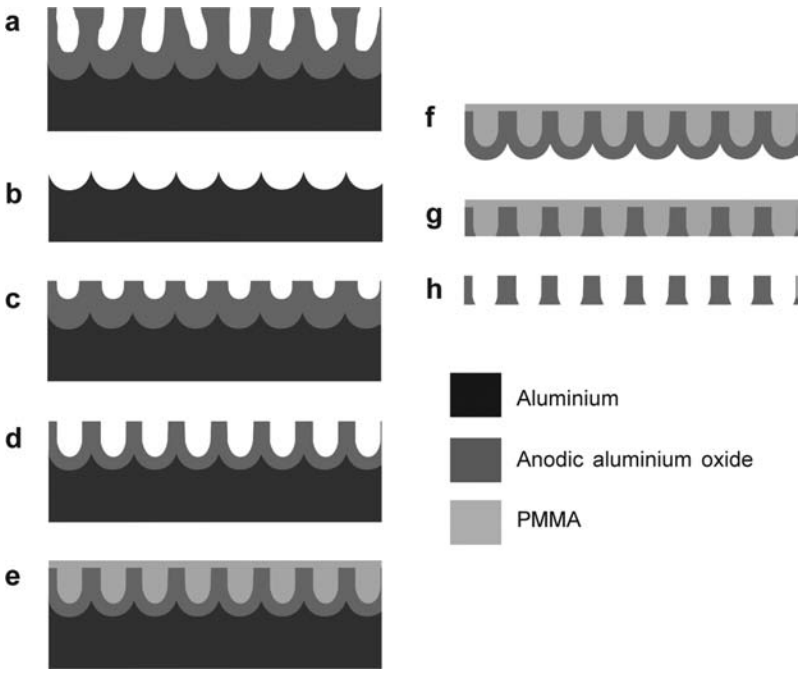

FIG. 1. Schematic drawing of the fabrication procedure of anodic aluminium oxide (AAO) thin films. (**a**) Formation of the porous alumina layer after the first anodization. (**b**) Removal of the anodic alumina layer using chemical etching. (**c**) Formation of the ordered porous alumina layer after the second anodization. (**d**) Chemical etching to widen the nanopores. (**e**) Removal of protective-layer coating and addition of polymethylmethacrylate to support the film. (**f**) Removal of the aluminium substrate. (**g**) Chemical etching to remove barrier layer oxide. (**h**) Removal of polymer support to afford nanoporous AAO.

(DMEM) supplemented with 10% fetal calf serum (FCS) (Invitrogen Gibco, Carlsbad, CA) and 1% penicillin/streptomycin (Invitrogen Gibco, Carlsbad, CA) at 37°C and 5% carbon dioxide (CO_2). Before experiments, cells were enzymatically lifted from tissue culture flasks using trypsin–ethylenediaminetetraacetic acid (Invitrogen Gibco, Carlsbad, CA), and the concentration of re-suspended cells was determined using a hemocytometer.

Keratinocyte and fibroblast adhesion to AAO membranes

AFM was used to qualitatively investigate the adhesion of keratinocytes to the inorganic AAO membrane. In two independent experiments, sterilized AAO membranes were brought into contact with HaCaT cell suspension (1×10^6 cells/mL) and imaged after 1 and 24 h of contact. The sample was thoroughly washed with fresh medium to remove any nonadhered cells and then quickly transferred to the AFM instrument and imaged under ambient laboratory conditions over a period of 2 h.

Separately, HaCaT cells were cultured on AAO membranes for 24 h and subsequently fixed for characterization using SEM. Samples were taken out of culture wells and washed thoroughly with phosphate buffered saline (PBS) before fixing in 3% glutaraldehyde and stained with 1% osmium tetroxide. After thorough washing in PBS and sequential dehydration in 50%, 70%, 95%, and 100% ethanol, samples were critical-point dried, sputter-coated in gold, and examined using SEM (Philips XL30).

Keratinocyte proliferation assay

Keratinocyte proliferation was investigated over 3 days of culture on each of the prepared membranes using a standard 3-(4,5-dimethylthiazol-2-yl)-5-(3-carboxymethoxypheny1)-2-(4-sulfophenyl)-2H-tetrazolium, innersalt (MTS) cell proliferation assay (Promega, Madison, WI), following the manufacturer's protocol. Triplicate membrane samples with differing nanopore sizes were cut to an exact size to cover the bottom of 24-well plates and ultraviolet light sterilized before freshly suspended cells were seeded at a density of 10^4 cells per well. At 0, 24, 48, and 72 h, samples were treated by adding the Promega Cell Titre Aqueous One Solution (MTS).[39] Samples were incubated for 3 h at 37°C and 5% CO_2, and absorbance was measured at 492 nm to determine cell number. Control samples with no membrane were also included.

Keratinocyte migration assay

Triplicate membrane samples were cut to an exact size to cover the bottom of 12-well plates and adhered with silicon

Table 1. Anodizing Conditions for the Fabrication of AAO Membranes with Different Pore Sizes

Anodizing acid	*Voltage*	*Time of first anodization (hours)*	*Time of second anodization (hours)*	*Pore size (nm)*
Oxalic acid (0.3 M)	30	7	14	60
Oxalic acid (0.3 M)	60	4	4	125
Sulfuric acid (0.3 M)	24	5	5	41
Phosphoric acid (2.5 M)	60	5	7	180–200
Phosphoric acid (0.3 M)	130	5	7	~500

glue. Glass slides were cut to fit the center of the wells and stood upright to provide a barrier to cell growth and thus a cell-free area for analysis of cell migration. HaCaT cells were labelled with CellTrace carboxyfluorescein succinimidyl ester (CFSE; Invitrogen Molecular Probes, Eugene, OR) to allow visualization of the cells on the opaque nanoporous membranes using fluorescent microscopy. Briefly, cells were suspended at 1×10^6 cells/mL in 0.1% bovine serum albumin/PBS and incubated with 10μM CFSE at 37°C for 10 min. Cells were thoroughly washed by repeated centrifugation and suspension in fresh medium (DMEM + 10% fetal bovine serum + 1% penicillin/streptomycin) and then seeded at a density of 2×10^5 cells/mL on the prepared 12-well plates. Plates were incubated at 37°C and 5% CO_2, and once the cell monolayer was confluent, the glass barriers were removed to reveal a cell-free area in the middle of the well. Wells were washed with PBS, and fresh medium was added. At 0, 12, 24, 36, 48, and 72 h, the cell-free area was photographed using a light microscope fixed with a 488-nm excitation source (Nikon Eclipse Inverted Microscope V1.21, final objective ×4, Melville, NY). Cell migration was measured by comparing the percentage of the image uncovered at each time point with the initial percentage using ImageJ software.[40]

Animal pilot study

The institutional animal ethics committee approved all animal experiments, which were performed in accordance with National Health and Medical Research Council Australian Code of Practice for the Care and Use of Animals for Scientific Purposes. Two large white juvenile pigs weighing 27 to 29 kg received a deep dermal partial-thickness burn on each flank, as previously described.[41] Wounds were dressed as test (with membrane) or control (Acticoat) and reviewed weekly for 4 weeks.

Statistical analyses

Differences in experimental groups were analyzed using unpaired *t*-test, with $p < 0.05$ as significant (StatView, V5.0.1, SAS Institute Inc., Cary, NC).

Results and Discussion

Nanoporous alumina membranes

Porous oxide growth on aluminium by anodic oxidation has been studied for more than 60 years. It is generally accepted that the production of a porous anodized film on

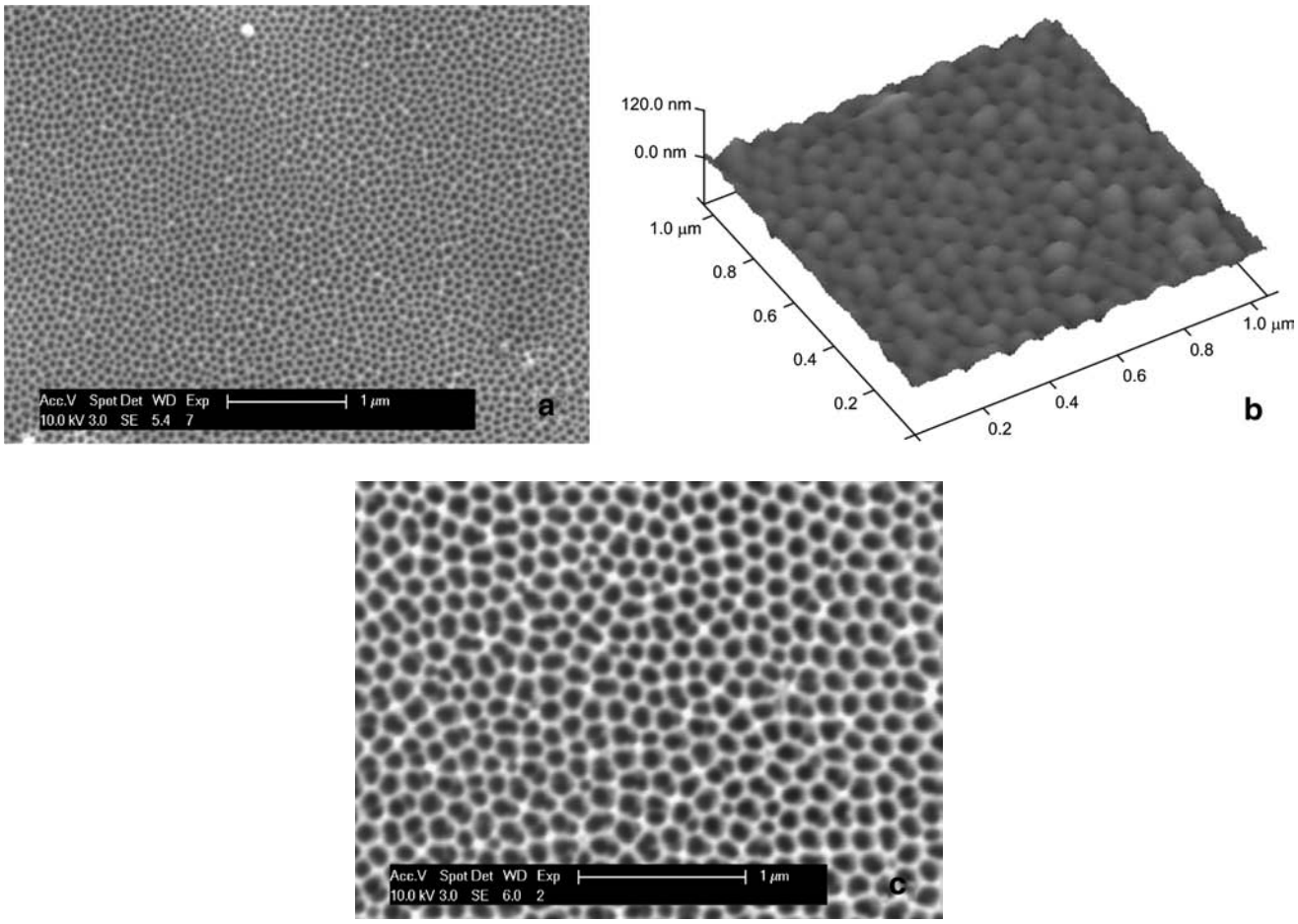

FIG. 2. (**a**) Scanning electron microscopy (SEM) image of top surface of AAO membrane prepared using a two-step anodization process in oxalic acid (0.3 M) at 30 V and 5°C. (**b**) Atomic force microscopy (AFM) scan depicting the three-dimensional surface topography of and lateral structure of the AAO membrane in (**a**). (**c**) SEM image of the top surface of anodic aluminium oxide membrane prepared using a two-step process in oxalic acid (0.3 M) at 60 V and 5°C.

aluminium requires a source of direct current and an acid solution that will provide oxygen ions. The passage of electric current causes decomposition of the acidic electrolyte, producing hydrogen at the cathode and promoting the attraction of negatively charged oxygen and electrolyte anions to the aluminium anode. The simultaneous drift of Al^{3+} ions from the substrate under the high-field conditions permits the formation of aluminium oxide at the anode surface.[42] O'Sullivan and Wood[43] attribute porous growth to an equilibrium of field-assisted oxide dissolution at the oxide–electrolyte interface and oxide growth at the metal–oxide interface. The field-assisted dissolution mechanism is based on the stretching and breaking of aluminium-oxygen bonds under the applied field, which proceeds at a faster rate than the open-field chemical dissolution of the film material. The field assists the rate of dissolution at the bottom of the pore to a greater extent than it assists growth and more than on the outer film surface, so that the pore can be propagated.[43] This model is able to give plausible explanations for the dependence of pore diameters and interpore distances on applied voltage or electrolyte composition. That is, field-assisted dissolution at the bottom of the pore will be further enhanced under a higher voltage, resulting in larger pores.[44]

Further advancements in the anodizing technology have seen the porous cell arrangement of AAO form an ideally packed hexagonal array by self-adjusting during an extended anodizing process.[31] Mechanistic studies have suggested that the self-organization is a result of repulsive forces between neighboring pores caused by mechanical stress associated with the expansion during oxide formation at the metal–oxide interface.[45] An advanced two-step anodization method is employed to fabricate straight and highly regular nanopore arrays that extend the length of the oxide film.[32] The porous oxide growth changes the surface of the aluminium substrate into a regular dimpled landscape that can act as a self-assembled template for a second anodization. As a result, the first anodic oxide layer is removed, and a subsequent anodization allows straight nano-channels to grow parallel through the oxide layer.

AAO membranes were characterized using SEM and AFM. Figure 2a is a SEM image of the surface topography of an AAO membrane prepared in oxalic acid at 30 V. The micrograph depicts nanopores existing in many ordered, hexagonal-patterned domains with highly regular and uniform pore sizes. The three-dimensional AFM scan in Figure 2b portrays the nanoporous topography to be investigated

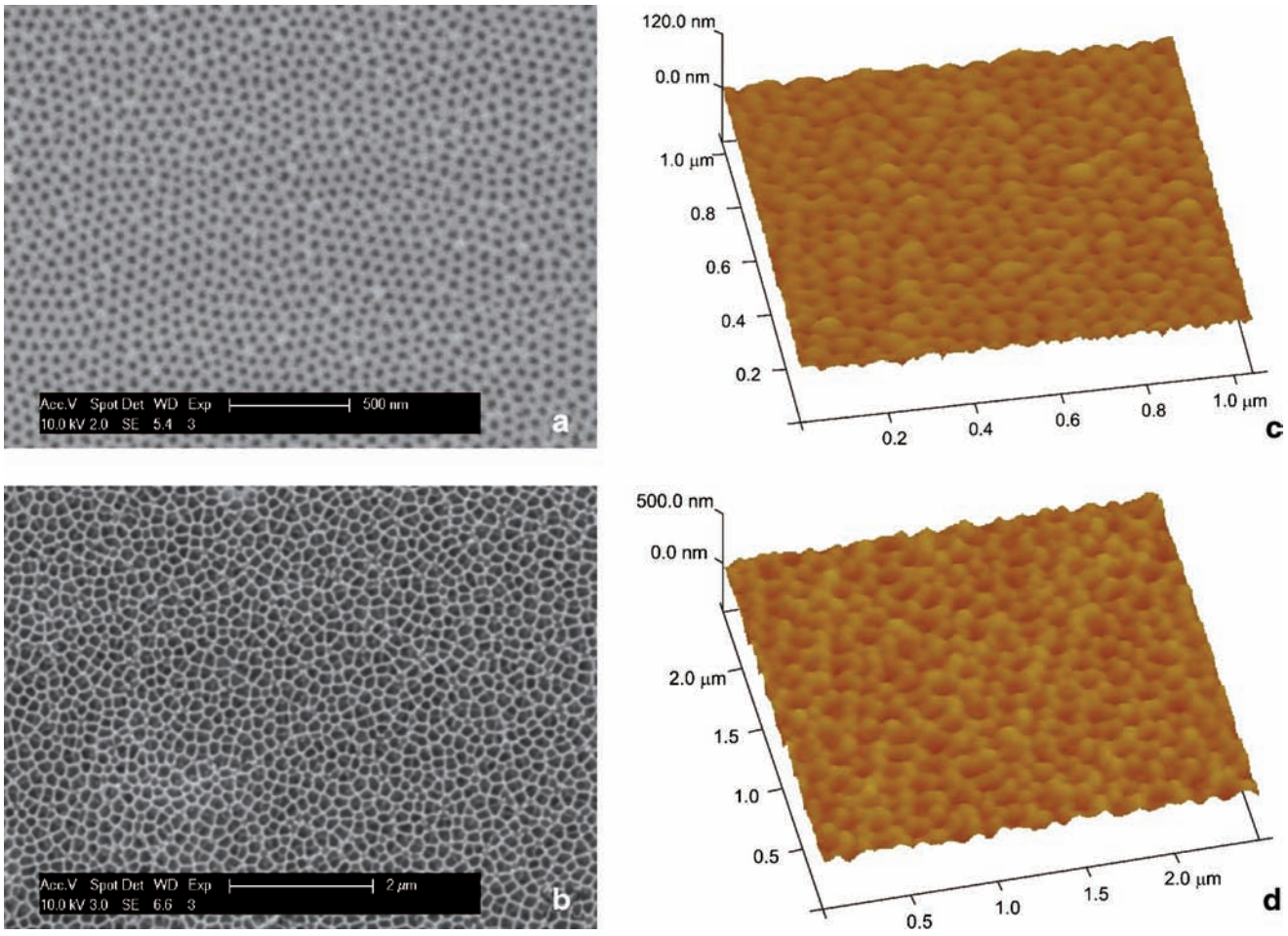

FIG. 3. (**a**) SEM image and (**b**) AFM scan of AAO membrane prepared using a two-step anodization process in sulfuric acid (0.3 M) at 24 V and 5°C. (**c**) SEM image and (**d**) AFM scan of AAO membrane prepared in phosphoric acid (2.5 M) at 60 V and 5°C. Color images available online at www.liebertonline.com/ten.

for skin cell response. Pore geometry was evaluated using sectional profile-line plots after imaging (ImageJ 1.40 g[40]). For the evaluation of the pore mouth diameter, profile marks were visually set on the upper inflexion points of the conical profile lines, and the interpore distance was measured by placing the marks in two adjacent minima of the same profile lines. The two-step anodization of aluminium in oxalic acid at 30 V produced pore mouth diameters of 60 ± 4 nm and interpore distances of 80 ± 3 nm. Figure 2c displays the surface topography of an AAO membrane prepared at a higher voltage (60 V) in oxalic acid. Pore geometry can be 'controlled' by changing the anodic electrolyte, the applied voltage, or both. Anodizing at a higher voltage produces a characteristically different membrane, with larger pores than those formed at 30 V. This is because of the enhanced-field dissolution of the oxide layer under the higher-forming voltage.[46] Again, the majority of pores exist in ordered domains and have an average pore mouth diameter of 125 ± 4 nm and an interpore distance of 155 ± 4 nm.

Figure 3 presents micrographs of AAO membranes prepared in sulfuric acid at 24 V (Fig. 3a, b) and phosphoric acid at 60 V (Fig. 3c, d). AFM surface scans illustrate the lateral structure of each of the membranes. Anodization in sulfuric acid yields a highly regular membrane, with almost all pores existing in large domains of hexagonal arrangement. These experimental conditions also yielded a membrane with the smallest pores, having an average pore mouth diameter of 41 ± 2.5 nm and an interpore distance of 64 ± 3 nm. The relatively unstable growth of aluminium oxide in phosphoric acid at 60 V resulted in membranes with pore sizes ranging from 90 to 270 nm, with the majority at 180 to 200 nm. These high-voltage conditions enhance dissolution of the oxide layer during anodization and induce a change in growth mechanism of the oxide film as described in [42]. Although the large and mostly noncylindrical pores deviate somewhat from the normal hexagonal arrangement, the nanoporous architecture was still present across the entire surface of the membrane. Finally, an AAO membrane prepared in phosphoric acid at 130 V provided nanopores of approximately500 nm in size.

Further optimization of the basic two-step anodization method has yielded membranes of superior quality and significant size, as depicted in Figure 4. AAO membranes manufactured using protocols based on previously described methods were flaky, delicate, and hard to recover as complete thin films (Fig. 4a). Our modified approach and custom-designed apparatus afforded highly reproducible membranes that could be recovered as complete films of improved quality, size (from $\sim$4.5–56 cm^2), and flexibility (Fig. 4b–e). Having only one side of the aluminium substrate exposed to anodization allowed the $CuCl_2$-based solution to have direct contact with the aluminium substrate, permitting a clean and fast removal without needing to penetrate and thus damage the overlaying AAO membrane. The use of the $CuCl_2$ solution to etch the aluminium substrate has an advantage over the commonly used mercuric chloride solution, because it provides faster removal and an environmentally friendly alternative that has no hazardous by-products or the potential to leave harmful residues on the membrane.[47] In addition, it was found that supporting the membrane with an acrylic film during the removal of the aluminium substrate made it much easier to recover a single large AAO membrane (Fig. 4c) of greater flexibility (Fig. 4e). They are also significantly larger than the commercially available Anopore alumina membranes at 14.5 cm^2 (Whatman, Maidstone, England) (Fig. 4d). Together, these optimized techniques allowed significant up-scaling of the AAO membranes to sizes that are practicable for larger-scale skin tissue engineering applications. It also demonstrates the capability of further up-scaling to even larger sizes. This is important for the potential clinical applications of the membrane as a dressing or template, because a large area of skin could be covered with one membrane.

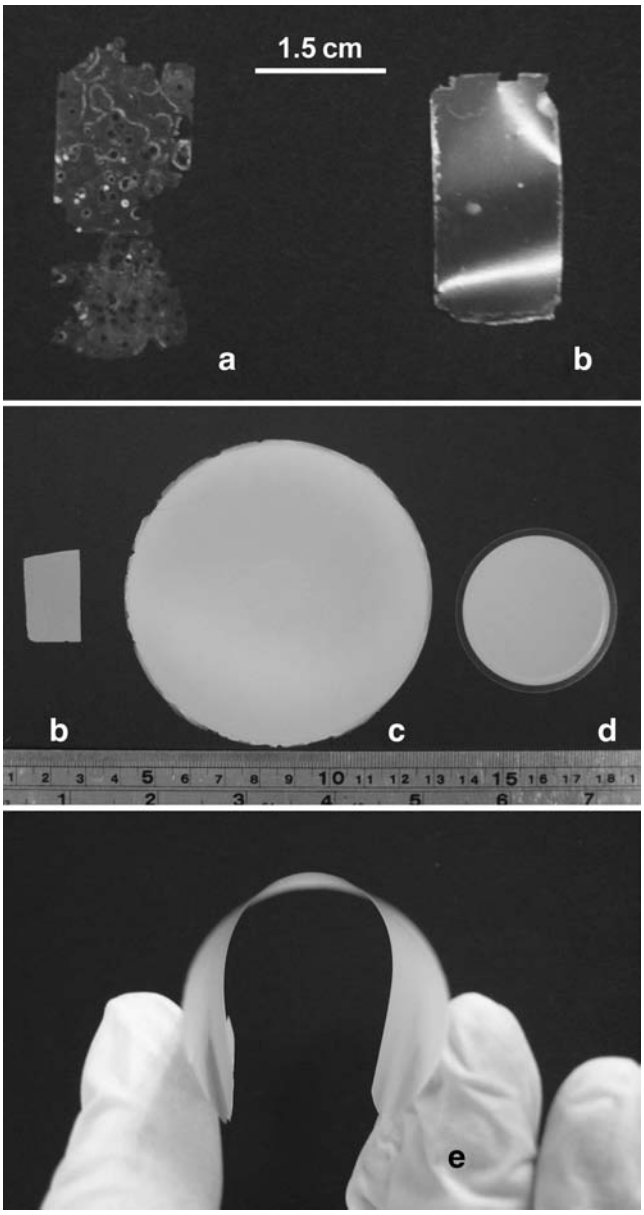

FIG. 4. Digital photographs illustrating the development of superior AAO membranes using an optimized fabrication method. (**a**) First membranes prepared based on previously described methods. (**b**) Fabrication of superior AAO membranes. (**c**) Large-scale, highly reproducible AAO membranes. (**d**) Commercially available Anopore alumina membrane. (**e**) Large-scale AAO membrane under manual mechanical stress depicting the flexibility of the membrane.

Cell adhesion

Two independent experiments were conducted to study the adhesion of keratinocytes on nanoporous AAO. Sterilized AAO membranes were placed in contact with a suspension of skin cells and then imaged after 1 and 24 h. AFM was employed for these studies because it is a nondestructive technique with the necessary resolution to characterize the underlying nanoporous substrate, as well as the cells on its surface.

AFM scans of a portion of AAO membrane that had been in contact with a freshly prepared skin cell suspension for 1 h show cells attached to the membrane (Fig. 5a). These appear as lighter masses on the darker membrane surface; keratinocytes had deposited onto the AAO substrate. The higher-resolution scans clearly indicate the presence of cells on the nanoporous membrane, where the highly ordered, hexagonal array of nanopores is evident below the mass of cells on its surface.

As part of the preparation of the sample for imaging, the membrane was thoroughly washed with fresh medium to remove any nonadhered cells from the sample. In addition, the deposition of cells onto the membrane was not due to sedimentation of the cells over time, because the membrane was not placed at the base of the cell suspension but rather was dipped into the suspension. This suggests that the cells were actively adhering through adhesion complexes to the membranes rather than sedimenting onto the surface. The stability of the cell attachment to the membrane under the AFM tip during contact mode scanning also suggests that

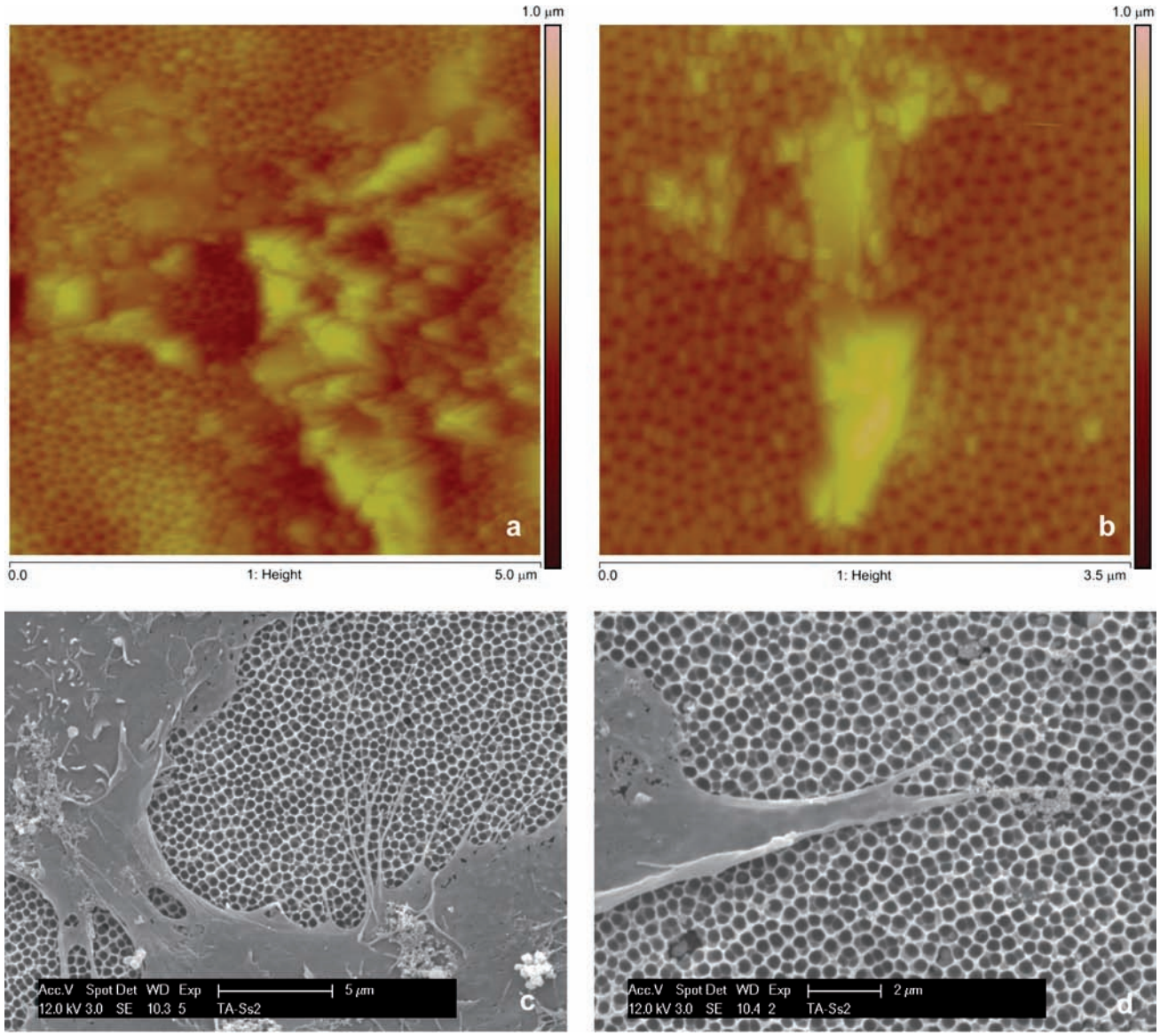

FIG. 5. (**a**) AFM scan of live HaCaT cells deposited on nanoporous anodic aluminium oxide after 1 h of contact with skin cell suspension, (**b**) after 24 h contact. AAO substrate was prepared from anodization in oxalic acid (0.3 M) at 60 V. Samples were prepared for imaging after washing thoroughly with fresh medium to remove any nonadhered cells. (**c** & **d**) SEM images of HaCaT cells on nanoporous AAO. Lamellipodia extending from the cell body can be seen to be of similar size to the pores, lying across the surface and protruding into the substrate. Color images available online at www.liebertonline.com/ten.

cells were strongly adhered, with reproducible scans achieved over different magnifications. AFM scans from macroscopically different areas of the sample depicted the deposition of cells across the entire surface of the membrane.

AFM imaging of the AAO membrane after 24 h of contact with the cell suspension was also performed. The images depict the continued interaction of cells on the surface of the membrane after 24 h (Fig. 5b). Reproducible AFM scans over different magnifications and different areas of the sample were obtained, and the observation of keratinocytes on the membrane after the extended period of time is a strong indication of firm attachment to the noncoated, inorganic substrate.

SEM analysis further supports the suggestion that the keratinocytes actively adhere through cell complexes (Fig. 5c, d). Here, cells were grown on a membrane for 24 h and then fixed for characterization using SEM. These images present evidence of a definite interaction between cells and the membrane at the nanolevel. Lamellipodia extending from the cell body can be seen to be of similar size to the pores, lying across the surface and protruding into the substrate (Fig. 5d).

To demonstrate that the attachment of cells to the membrane was not only a property of the keratinocyte cell type, we also used NIH-3T3 fibroblasts and monitored attachment of these cells to the membrane. As with the keratinocytes, consistent adhesion of these cells to the membranes was observed at 1 and 24 h after incubation (data not shown), suggesting that cell attachment to the membrane is a property of multiple cell types.

The membrane appears to provide a landscape for the cells to engage with for firm attachment, and it is hoped that, by exploiting this interaction at the nanoscale, we may potentially alter cell behavior to promote faster wound healing.

Proliferation and migration

Our adhesion studies of cells on AAO films demonstrate cell attachment to the inorganic nanoporous membranes but do not provide information on the long-term viability or proliferative potential of these cells or the motility of the cells across the surface. These properties are important in the context of developing biological scaffolds or templates for tissue engineering. Additionally, it is important to determine whether changes to nanopore size affect cell behavior. A proliferation assay was performed to quantify the growth of keratinocytes across each of the different nanoporous membranes. As in all experiments, the inert, inorganic membranes were used as prepared, with no further chemical or physical surface modifications. The results of the 3-day proliferation assay suggest that there is an effect of nano-architecture on

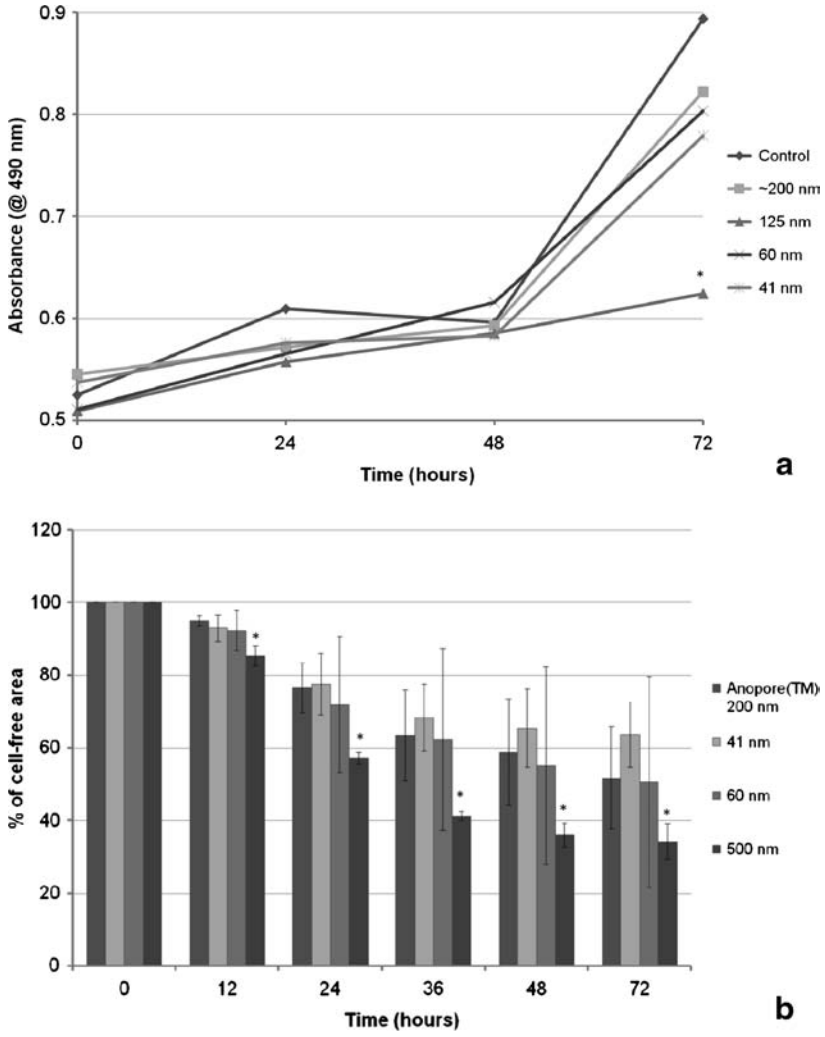

FIG. 6. (**a**) Results of 3-day MTS proliferation assay of HaCaT cells on the prepared nanoporous AAO membranes. There was a significant difference ($^*p < 0.05$) in proliferation on the membrane of 125-nm pores than on the control and other membranes. (**b**) Results of HaCaT migration on nanoporous AAO membranes. There was an effect of nano-architecture on cell migration, with cells migrating significant faster ($^*p < 0.05$) on the 500-nm membrane than on the 65-nm and the commercially available Anopore membranes.

keratinocyte growth (Fig. 6a). There were significantly fewer cells ($p < 0.05$) in culture at Day 3 growing on the membrane of 125-nm pores than on the control and other AAO membranes. Although this particular interpore distance appears to inhibit cell proliferation, which is unlikely to be desired during the acute tissue repair phase, it demonstrates that keratinocyte cells are sensitive to changes in the nanoscale topography of these membranes.

In addition there was an effect of nano-architecture on cell motility (Fig. 6b). HaCaT cell migration was investigated over four different nanoporous membranes, one of which was the commercially available Anopore alumina membrane (Whatman). A 'cell-free area' was created in a confluent cell layer, and migration of cells to cover the gap was monitored. Cells migrated faster ($p < 0.05$) across the membrane with 500-nm pores than across the 65-nm and 200-nm Anopore membranes. At 24 h and all following time points, the closure of the 'gap' on the 500 nm was significantly faster ($p = 0.049$, $p = 0.03$, $p = 0.04$, $p = 0.03$, respectively) than on the 65-nm membranes, and at 12 and 24 h, migration was faster ($p = 0.01$ and $p = 0.03$, respectively) on the 500-nm membrane than the Anopore membrane.

The potential of AAO membranes in skin repair

Changes in the surface nano-architecture influence keratinocyte behavior, and further testing of different pore sizes and arrangements may optimize a membrane for rapid growth of the epithelial layer and enhance cutaneous repair after injury.

Alternatively, inhibition of cells migrating into the wound that cause scarring may be a potential use for these templates. This is the first reported investigation into the effects of AAO on skin cell types, and we propose that the membrane may be used to enhance healing by promoting migration and proliferation of epithelial cells across the membrane surface when applied as a topical dressing to a wound, thereby promoting faster wound closure and consequently reducing scarring.[1] For this application to be possible, the membrane will need to conform to the skin surface and be nondegradable in the wound environment, and the attachment of cells to the membrane surface must be weaker than to each other, such that removal of the membrane 'dressing' will not remove the nascent epithelial layer. We have tested whether the physical properties of the AAO membranes may be suitable for this type of application. A pilot study involving the application of sample AAO membranes to a topical, dorsal flank burn injury in the pig demonstrated adherence and conformability of the membranes to the wound surface, with no observed degradation over a period of 3 weeks (Fig. 7). Membranes were also able to be removed without loss of the forming epidermis, with no detrimental effect on the wound healing process. This pilot application of the membranes *in vivo* suggests that the application of AAO membranes as topical dressings to skin injuries is feasible. In light of this pilot study, and the *in vitro* results presented here, we intend to conduct an *in vivo* trial using a porcine burn injury model.[41] This will allow extensive assessment of wound closure rates with changing pore sizes, as well as an opportunity to assess any effects of AAO membranes on other important wound healing processes, for example, inflammation, that are not easily assessed *in vitro*.

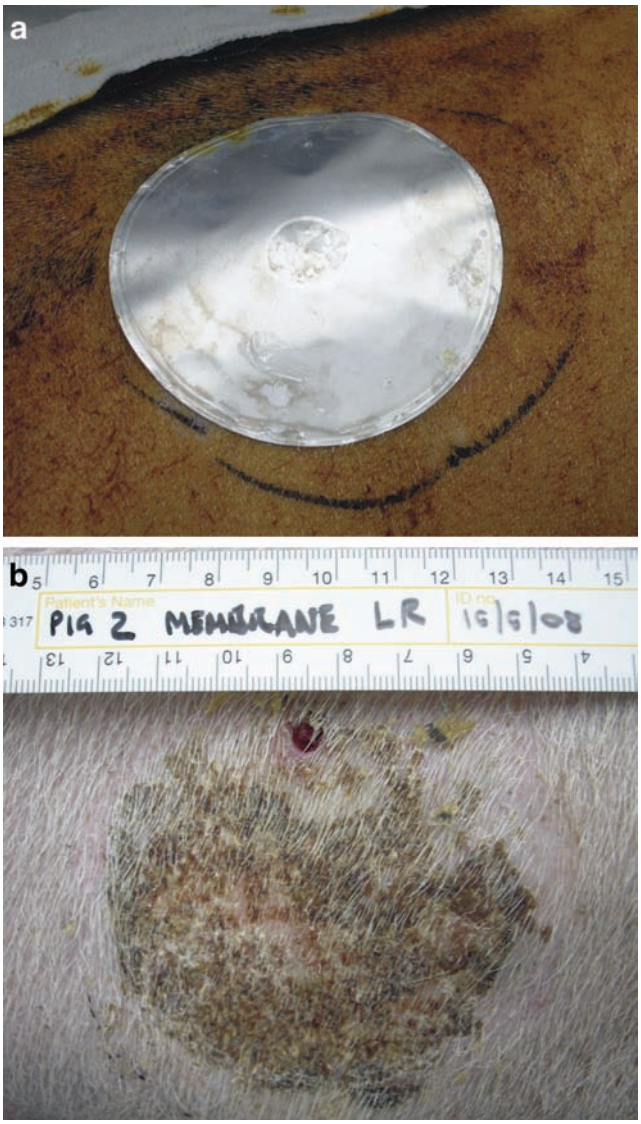

FIG. 7. Potential use of AAO membrane as a dressing for skin wound healing. (**a**) Membrane (with aluminium backing for support) conforms to skin surface when applied to a burn injury in the pig. (**b**) Removal of membrane does not appear to disrupt surface repair. Color images available online at www.liebertonline.com/ten.

Conclusion

Here, we have shown that skin cell types attach, are viable, proliferate, and migrate over a period of days on AAO membranes, with an effect of surface nanotopography on cell behavior. Also, the better performance and larger size than the commercially available Anopore membrane suggests that our optimized fabrication process produces more-favorable nanoporous architecture for keratinocyte function and membranes of sufficient size for wound-healing applications.

This work demonstrated that changes to surface nanotopography can influence skin cell behavior, with significant differences in cell proliferation and migration depending on pore size. The reproducibility, uniformity, biocompatibility, physical properties, and cost of the AAO membranes make them potentially suitable for clinical application. Further

investigation into the mechanism by which nanotopography affects cell behavior, together with an *in vivo* study assessing the effects of these membranes on skin wound healing, may lead to better tissue engineering substrates for skin and other tissue repair.

Disclosure Statement

No competing financial interests exist.

References

1. Deitch, E.A., Wheelahan, T.M., Rose, M.P., Clothier, J., Cotter, J. Hypertrophic burn scars: analysis of variables. J Trauma **23,** 895, 1983.
2. Geiger, B., Bershadsky, A., Pankov, R., Yamada, K.M. Transmembrane extracellular matrix-cytoskeleton crosstalk. Nat Rev Mol Cell Biol **2,** 793, 2001.
3. Lo, C.-M., Wang, H.-B., Dembo, M., Wang, Y.-l. Cell movement is guided by the rigidity of the substrate. Biophys J **79,** 144, 2000.
4. Huang, S., Ingber, D.E. The structural and mechanical complexity of cell-growth control. Nat Cell Biol **1,** E131, 1999.
5. Pham, C., Greenwood, J., Cleland, H., Woodruff, P., Maddern, G. Bioengineered skin substitutes for the management of burns: a systematic review. Burns **33,** 946, 2007.
6. Yannas, I.V., Burke, J.F., Orgill, D.P., Skrabut, E.M. Wound tissue can utilize a polymeric template to synthesize a functional extension of skin. Science **215,** 174, 1982.
7. Orgill, D.P., Straus II, F.H., Lee, R., C. The use of collagen-GAG membranes in reconstructive surgery. Ann N Y Acad Sci **888,** 233, 1999.
8. Trent, J.F., Kirsner, R.S. Tissue engineered skin: Apligraf, a bi-layered living skin equivalent. Int J Clin Pract **52,** 408, 1998.
9. Singhvi, R., Stephanopoulos, G., Wang, D.I.C. Review: effects of substratum morphology on cell physiology. Biotechnol Bioeng **43,** 764, 1994.
10. Clark, P., Connolly, P., Curtis, A.S.G., Dow, J.A.T., Wilkinson, C.D.W. Cell guidance by ultrafine topography in vitro. J Cell Sci **99,** 73, 1991.
11. Flemming, R.G., Murphy, C.J., Abrams, G.A., Goodman, S.L., Nealey, P.F. Effects of synthetic micro- and nano-structured surfaces on cell behaviour. Biomaterials **20,** 573, 1999.
12. Teixeira, A.I., Abrams, G.A., Bertics, P.J., Murphy, C.J., Nealey, P.F. Epithelial contact guidance on well-defined micro- and nanostructured substrates. J Cell Sci **116,** 1881, 2003.
13. Curtis, A., Wilkinson, C. Nantotechniques and approaches in biotechnology. Trends Biotechnol **19,** 97, 2001.
14. Wilkinson, C.D.W., Riehle, M., Wood, M., Gallagher, J.O., Curtis, A.S.G. The use of materials patterned on a nano- and micro-metric scale in cellular engineering. Mater Sci Eng C **19,** 263, 2002.
15. Andersson, A.-S., Backhed, F., von Euler, A., Richter-Dahlfors, A., Sutherland, D., Kasemo, B. Nanoscale features influence epithelial cell morphology and cytokine production. Biomaterials **24,** 3427, 2003.
16. Smith, L.A., Ma, P.X. Nano-fibrous scaffolds for tissue engineering. Colloids Surf B Biointerfaces **39,** 125, 2004.
17. Wan, Y., Wang, Y., Lui, Z., Qu, X., Han, B., Bei, J., Wang, S. Adhesion and proliferation of OCT-1 osteoblast-like cells on micro- and nano-scale topography structured poly(L-lactide). Biomaterials **26,** 4453, 2005.
18. Dalby, M.J., Pasqui, D., Affrossman, S. Cell response to nano-islands produced by polymer demixing: a brief review. IEE Proc Nanobiotechnol **151,** 53, 2004.
19. Norman, J.J., Desai, T.A. Methods for fabrication of nanoscale topography for tissue engineering scaffolds. Ann Biomed Eng **34,** 89, 2006.
20. Sachlos, E., Czernuszka, J.T. Making tissue engineering scaffolds work. Review on the application of solid freeform fabrication technology to the production of tissue engineering scaffolds. Eur Cells Mater **5,** 29, 2003.
21. Gupta, A., Seifalian, A.M. Novel electrohydrodynamic printing of nanocomposite biopolymer scaffolds. J Bioact Compat Polym **22,** 265, 2007.
22. Chen, F., Lee, C.N., Teoh, S.H. Nanofibrous modification on ultra-thin poly(e-caprolactone) membrane via electrospinning. Mater Sci Eng C **27,** 325, 2007.
23. Kothapalli, C.R., Shaw, M.T., Wei, M. Biodegradable HA-PLA 3-D porous scaffolds: effect of nano-sized filler content on scaffold properties. Acta Biomater **1,** 653, 2005.
24. Shum, A.W.T., Li, J., Mak, A.F.T. Fabrication and structural characterization of porous biodegradable poly(DL-lactic-co-glycolic acid) scaffolds with controlled range of pore sizes. Polym Degrad Stab **87,** 487, 2005.
25. Karlsson, M., Johansson, A., Tang, L., Boman, M. Nanoporous aluminum oxide affects neutrophil behaviour. Microsc Res Tech **63,** 259, 2004.
26. Karlsson, M., Palsgard, E., Wilshaw, P.R., Di Silvio, L. Initial in vitro interaction of osteoblasts with nano-porous alumina. Biomaterials **24,** 3039, 2003.
27. Popat, K.C., Swan, E.E.L., Mukhatyar, V., Chatvanichkul, K.-I., Mor, G.K., Grimes, C.A., Desai, T.A. Influence of nanoporous alumina membranes on long-term osteoblast response. Biomaterials **26,** 4516, 2005.
28. Swan, E.E.L., Popat, K.C., Desai, T.A. Peptide-immobilized nanoporous alumina membranes for enhanced osteoblast adhesion. Biomaterials **26,** 1969, 2005.
29. Swan, E.E.L., Popat, K.C., Grimes, C.A., Desai, T.A. Fabrication and evaluation of nanoporous alumina membranes for osteoblast culture. J Biomed Mater Res A **72,** 288, 2005.
30. Hoess, A., Teuscher, N., Thormann, A., Aurich, H., Heilmann, A. Cultivation of hepatoma cell line HepG2 on nanoporous aluminum oxide membranes. Acta Biomater **3,** 43, 2007.
31. Masuda, H., Fukuda, K. Ordered metal nanohole arrays made by a two-step replication of honeycomb structures of anodic alumina. Science **268,** 1466, 1995.
32. Masuda, H., Satoh, M. Fabrication of gold nanodot array using anodic porous alumina as an evaporation mask. Jpn J Appl Phys **35,** L126, 1996.
33. Li, A.P., Muller, F., Birner, A., Nielsch, K., Gosele, U. Hexagonal pore arrays with a 50–420 nm interpore distance formed by self-organization in anodic alumina. J Appl Phys **84,** 6023, 1998.
34. Ono, S., Saito, M., Asoh, H. Self-ordering of anodic porous alumina formed in organic acid electrolytes. Electrochim Acta **51,** 827, 2005.
35. Wang, X., Han, G.-R. Fabrication and characterization of anodic aluminium oxide template. Microelectronic Eng **66,** 166, 2003.
36. Hamadouche, M., Boutin, P., Daussange, J., Bolander, M.E., Sedel, L. Alumina-on-alumina total hip arthroplasty: a minimum 18.5-year follow-up study. J Bone Jt Surg **84,** 69, 2002.
37. Webster, T.J., Siegel, R.W., Bizios, R. Design and evaluation of nanophase alumina for orthopaedic/dental applications. Nanostructured Mater **12,** 983, 1999.

38. Boukamp, P., Petrussevska, R.T., Breitkreutz, D., Hornung, J., Markham, A., Fusenig, N.E. Normal keratinization in a spontaneously immortalized aneuploid human keratinocyte cell line. J Cell Biol **106,** 761, 1988.
39. Promega. Cell Titre 96 Aqueous One Solution Cell Proliferation Assay. Technical Bulletin Part #TB245 www .promega.com, 2005.
40. Rasband, W. Image J 1.40g, National Institutes of Health, Bethesda, MD. http://rsb.info.nih.gov/ij/, Java 1.6.0_05.
41. Cuttle, L., Kempf, M., Phillips, G.E., Mill, J., Hayes, M.T., Fraser, J.F., Wang, X.-Q., Kimble, R.M. A porcine deep dermal partial thickness burn model with hypertrophic scarring. Burns **32,** 806, 2006.
42. Vrublevsky, I., Parkoun, V., Schreckenbach, J. Analysis of porous oxide film growth on aluminium in phosphoric acid using re-anodizing technique. Appl Surf Sci **242,** 333, 2005.
43. O'Sullivan, J.P., Wood, G.C. The morphology and mechanism of formation of porous anodic films on aluminium. Proc R Soc Lond A Math Phys Sci **317,** 511, 1970.
44. Ghorbani, M., Nasirpouri, F., Iraji zad, A., Saedi, A. On the growth sequence of highly ordered nanoporous anodic aluminium oxide. Mater Des **27,** 983, 2006.
45. Jessensky, O., Muller, F., Gosele, U. Self-organized formation of hexagonal pore arrays in anodic alumina. Appl Phys Lett **72,** 1173, 1998.
46. Vrublevsky, I., Parkoun, V., Schreckenbach, J., Marx, G. Study of porous oxide film growth on aluminium in oxalic acid using a re-anodizing technique. Appl Surf Sci **227,** 282, 2004.
47. Zhao, Y., Chen, M., Zhang, Y., Xu, T., Lui, W. A facile approach to formation of through-hole porous anodic aluminium oxide film. Mater Lett **59,** 40, 2005.

Address correspondence to:
Leigh G. Parkinson, B.Sc.(Hons)
Physics and Nanoscience, School of Engineering and Energy
Murdoch University
Murdoch, WA 6150

E-mail: l.parkinson@murdoch.edu.au

Received: October 26, 2008
Accepted: May 22, 2009
Online Publication Date: August 27, 2009